Applied Microbiology and Biotechnology (2022) 106:2739–2750
https://doi.org/10.1007/s00253-022-11850-0

ENVIRONMENTAL BIOTECHNOLOGY

Changes in physiological states of *Salmonella* Typhimurium measured by qPCR with PMA and DyeTox13 Green Azide after pasteurization and UV treatment

Liyan Li[1] · Jing Fu[2] · Sungwoo Bae[1]

Received: 26 August 2021 / Revised: 17 January 2022 / Accepted: 26 February 2022 / Published online: 9 March 2022

Abstract

Diarrheal diseases caused by *Salmonella* pose a major threat to public health, and assessment of bacterial viability is critical in determining the safety of food and drinking water after disinfection. Viability PCR could overcome the limitations of traditional culture-dependent methods for a more accurate assessment of the viability of a microbial sample. In this study, the physiological changes in *Salmonella* Typhimurium induced by pasteurization and UV treatment were evaluated using a culture-based method, RT-qPCR, and viability PCR. The plate count results showed no culturable *S.* Typhimurium after the pasteurization and UV treatments, while viability PCR with propidium monoazide (PMA) and DyeTox13-qPCR indicated that the membrane integrity of *S.* Typhimurium remained intact with no metabolic activity. The RT-qPCR results demonstrated that invasion protein (*invA*) was detectable in UV-treated cells even though the log2-fold change ranged from − 2.13 to − 5.53 for PMA treatment. However, the catalytic activity gene *purE* was under the detection limit after UV treatment, indicating that most *Salmonella* entered metabolically inactive status after UV disinfection. Also, viability PCRs were tested with artificially contaminated eggs to determine physiological status on actual food matrices. DyeTox13-qPCR methods showed that most *Salmonella* lost their metabolic activity but retained membrane integrity after UV disinfection. RT-qPCR may not determine the physiological status of *Salmonella* after UV disinfection because mRNA could be detectable in UV-treated cells depending on the choice of target gene. Viability PCR demonstrated potential for rapid and specific detection of pathogens with physiological states such as membrane integrity and metabolic activity.

Key Points

- *Membrane integrity of Salmonella remained intact with no metabolic activity after UV.*
- *mRNA could be detectable in UV-treated cells depending on the choice of target gene.*
- *Viability PCR could rapidly detect specific pathogens with their physiological states.*

Keywords Viability PCR · *Salmonella* · VBNC · DyeTox13-qPCR

Introduction

Acute diarrheal disease remains a major public health issue, with 555 million people falling ill every year according to the World Health Organization, including 220 million children under the age of five (World Health 2021). Salmonellosis is a globally common diarrheal disease caused by *Salmonella*, a zoonotic and Gram-negative pathogenic bacterium. The ubiquitous distribution of *Salmonella* in nature makes its infection a global human health issue (Majowicz et al. 2010), and contaminations of food matrices such as milk, eggs, and produce with *Salmonella* have been reported in Singapore and worldwide (Majowicz et al. 2010; Sánchez-Vargas, Abu-El-Haija et al. 2011, Aung et al. 2020).

Thermal and nonthermal technologies (e.g., ultraviolet (UV) irradiation) have been used to ensure the microbiological safety of food and water. Traditional methods for isolating and identifying *Salmonella* rely on enrichment followed by isolation using selective and differential media

✉ Sungwoo Bae
ceebsw@nus.edu.sg

[1] Department of Civil and Environmental Engineering, National University of Singapore, 1 Engineering Drive 2, Singapore 117576, Singapore

[2] Key Laboratory of Organic Compound Pollution Control Engineering, School of Environmental and Chemical Engineering, Shanghai University, Shanghai, China

(Zhang et al. 2015). However, culture-dependent approaches are time-consuming and might potentially result in false negatives due to the presence of "viable but nonculturable" (VBNC) cells that could be produced by sublethal heat (pasteurization), UV treatment, and autoclave sterilization (heat-lysis) (Zhao et al. 2017; Lee and Bae 2018a, b). Alternatively, molecular detection methods such as PCR have been applied for rapid detection of *Salmonella*. Despite its speed, sensitivity, and specificity, the major disadvantage of the PCR approach is its inability to discriminate dead from live bacteria, hence the presence of dead bacteria leading to false-positive results.

Viability PCR has been developed to overcome the above limitations by rapidly and selectively quantifying viable cells using DNA-intercalating dyes such as ethidium monoazide (EMA) and propidium monoazide (PMA) (Bae, Wuertz et al. 2009). Both EMA and PMA are membrane-impermeant and can selectively bind to the DNA of dead cells whose cell membranes have been compromised. After photo-activation, EMA or PMA binds covalently to nucleic acids and inhibits DNA amplification of DNA from membrane-compromised cells during the PCR reactions. DyeTox13 Green C-2 Azide (DyeTox13), a newly developed DNA-intercalating dye, is also membrane-permeant and can selectively detect only viable cells that have enzymatic activity. In principle, DyeTox13 binds to the nucleic acids of dead and enzymatically inactive cell with intact membrane to prevent PCR amplification, while the nucleic acids of metabolically active cells can be amplified by PCR polymerase because the intracellular esterase enzyme activity cleaves the azide group in DyeTox13 (Lee and Bae 2018a, b, Chiang et al. 2021).

Recognizing that culturability is not the best proxy for cell viability, the detection of bacterial transcripts has been proposed as an indicator of cell viability due to the short half-lives and high turnover rates of mRNAs. It has been assumed that mRNA levels rapidly decrease after cell death because bacterial transcripts are sensitive to degradation by intra- and extra-cellular RNases (Kort et al. 2008; Trevors 2012; Ju et al. 2016). Therefore, reverse-transcription quantitative PCR (RT-qPCR) assays have been used to detect foodborne pathogens such as enterohemorrhagic *E. coli*, *Listeria monocytogenes*, *Salmonella*, and *Campylobacter* species (Rodriguez-Lazaro et al. 2006). However, transcript detection is not always correlated with the presence of viable cells (Kort et al. 2008), and continued gene expression after cell death in bacteria has been reported to limit the value of RT-qPCR for viability assessment (Trevors 2012). For example, all VBNC *E. coli* O157:H7 retained expression of Shiga-like toxin in river water, buffer, deionized water, and chloraminated treated water (Trevors 2011), and *E. coli* and *Pseudomonas putida* cells have demonstrated gene expression in milk after pasteurization (Gunasekera et al. 2002). Also, RNA from dead *E. coli* O157:H7 and RNaseA-treated *E. coli* was amplified by RT-qPCR, demonstrating that gene expression can continue in dead bacteria cells for limited periods of time (Ju et al. 2016).

Determining the viability of microbial samples is one of the most routine tasks in a microbiological laboratory. The viability of microorganisms is crucial in determining the safety of food and drinking water and has critical implications in the fields of environmental and medical microbiology. However, the term 'viability' is complex and often difficult to define, as it can refer to several characteristics, such as culturability, intact cell membrane, and metabolic activity. Since each method for determining cell viability is based on criteria that reflect different levels of cellular integrity or functionality, this study aimed to evaluate changes in the physiological characteristics of pathogenic *Salmonella enterica* Typhimurium induced by pasteurization and UV treatment. Specifically, we employed different detection methods representing culturability, membrane permeability, mRNA contents, and metabolic activity. Thus, the objectives of this study were to (1) to optimize the DyeTox13 assay with EMA to reduce the PCR signal from dead cells in the Gram-negative bacteria *S.* Typhimurium; (2) to investigate physiological changes of *S.* Typhimurium cell's condition induced by pasteurization and UV disinfection using RT-qPCR, PMA-qPCR, DyeTox13-qPCR, and a plate counting method; and (3) to test the DyeTox13-vPCR approach in monitoring *S.* Typhimurium on the surface of contaminated eggshells after pasteurization and UV treatment.

Materials and methods

Bacteria strains and growth conditions

Salmonella enterica serovar Typhimurium ATCC 14028 (*S. typhimurium*) was used as a model organism to study the effects of pasteurization and UV irradiation on cell viability criteria such as culturability, membrane integrity, metabolic activity, and gene expression. A single colony from the overnight Tryptic Soy (Difco™, USA) agar plate of *S.* Typhimurium was transferred to 100 mL of sterile tryptic soy broth (TSB, Sigma-Aldrich, USA) and incubated for 12 h at 37 °C with shaking at 150 rpm. The cells were then washed and resuspended in 50 mL 1 × phosphate-buffered saline (1 × PBS). The final concentration of *S.* Typhimurium was adjusted to OD_{600} equal to 0.25 (approximately 10^7 to 10^8 CFU/mL) for the following experiments.

Heat-lysis, pasteurization, and UV disinfection

Before PMA, DyeTox13, and DyeTox13 + EMA treatment, the suspensions of *S.* Typhimurium were treated with either heat-lysis, pasteurization, or UV disinfection. In the

heat-lysis treatment, *S.* Typhimurium suspensions in 500 µL 1 × PBS (OD_{600} = 0.25) were heated at 95 °C for 15 min on a standard laboratory heat block (Bio Laboratories, Singapore). The cells were then immediately placed on ice for 5 min until they reached room temperature. The loss of viability was determined in triplicate by spreading 100 µL of heat-killed cells on TSA plates.

For pasteurization, the same condition of *S.* Typhimurium suspensions in 500 µL 1 × PBS was heated to 63 ℃ for 30 min. After this step, samples were kept cool by placing them on ice before the dye treatments. UV disinfection experiments were conducted on 5 mL of bacterial suspensions (1 × PBS, OD_{600} = 0.25) in 30-mm Petri dishes with fully covering the base of Petri dish. The Petri dishes were placed in a Type A2 Biological Safety Cabinet (BSC) equipped with a timed UV system (Thermo Scientific), where the intensity of the UV disinfection was maintained at 0.055 mW/cm^2 as tested by a standard laboratory radiometer (IL 1400A Radiometer, International Light). UV exposure times of 10, 20, and 30 min were applied, equivalent to 33, 66, and 99 mJ/cm^2, respectively. Cells suspended in 1 × PBS buffer without UV treatment were tested in parallel as a control in the following dye experiments. For both pasteurization and UV-treated cells, the loss of cell culturability was determined in triplicate by plate counting on TSA.

PMA, DyeTox13, and DyeTox13+EMA treatments

Propidium monoazide (PMA, Biotium, Hayward, CA, USA), DyeTox13 Green C-2 Azide (DyeTox13, Setareh Biotech, OR, USA), and ethidium monoazide bromide (EMA, Biotium, USA) were dissolved in 20% dimethyl sulfoxide (DMSO, Sigma-Aldrich, Singapore) to obtain a 20 mM stock solution and stored at − 20 °C in the absence of light. Each 500-µL aliquot of cell suspension was treated with either PMA or DyeTox13 to obtain a final concentration of 50 µM based on previous studies (Bae, Wuertz et al. 2009; Lee and Bae 2018a, b; Lee and Bae 2018a, b). In addition, DyeTox13 and EMA were added together to create a third co-treatment of DyeTox13 + EMA assay, in which DyeTox13's final concentration remained 50 µM while EMA's final concentration was adjusted to 10, 25, and 50 µM separately. After the addition of the dyes, cell suspensions were mixed well by vortex and then incubated in the dark at room temperature for 10 min. Subsequently, the samples were exposed to intense visible light for 15 min using a PMA-Lite™ LED photolysis device (Biotium, Inc., CA, USA). The maximum temperature measured for PMA-Lite™ LED photolysis exposure was at 38.2 °C, which is close to the bacterial culture temperature. Thus, the additional heat generated during PMA-Lite exposure can be ignored. The dye-treated samples were then pelleted by centrifugation for DNA extraction (5000 × g for 10 min) and RNA extraction (5000 × g for 5 min).

DNA and RNA extraction

Genomic DNA (gDNA) was extracted from the 500-µL dye-treated and untreated samples using a GeneJET Genomic DNA Purification Kit (Thermo Fisher Scientific, Wilmington, DE, USA) according to the manufacturer's instructions. The concentrations of DNA were determined using a NanoDrop 2000 spectrophotometer (Thermo Fisher Scientific, USA).

Before RNA extraction, the RNA Protect Bacterial Reagent (Qiagen, Valencia, CA, USA) was added to stabilize the total RNA in the bacterial cultures. RNA extraction was subsequently performed using a PureLink RNA Mini Kit (Ambion, Life Technologies, USA) according to the manufacturer's protocol. The eluted RNAs were treated with an on-column PureLink DNase Kit (Ambion, Life Technologies, USA) to remove residual contaminating DNA before cDNA synthesis. We determined the amount of RNA present using the NanoDrop 2000 spectrophotometer.

cDNA synthesis and quantitative PCR assays

The *invA* (Invasion protein InvA) and *purE* (phosphoribosylaminoimidazole carboxylase) genes were selected to understand bacteria detection and metabolic activity in this study. The *invA* gene, an essential component of the invasion-associated protein secretion apparatus, contains unique sequences specific to the genus *Salmonella* and has been used as a target gene in both PCR and qPCR assays (Kidgell et al. 2002; Chen et al. 2011; Yang et al. 2018). The *purE* gene was used to examine the metabolic activity of bacteria cells because of its involvement in nucleotide biosynthesis (Karlinsey et al. 2019). cDNA was synthesized from 10 ng of total RNA using a SuperScript IV Reverse Transcriptase (Thermo Fisher Scientific). The primers used in this study are listed in Table S1, including the primer sequences, the optimal Tm, and the amplicon sizes of the target genes. Quantitative PCR (qPCR) assays were performed to amplify both gDNA and cDNA in a MicroAmp optical 96-well reaction plate using an automated ABI Step-One-Plus Real-Time PCR system (Applied Biosystems, CA, USA). Each of the 20-µL qPCR reactions (applied in triplicate) contained 2 µL of gDNA or cDNA, 10 µL of 2 × PowerUp SYBR® Green PCR Master Mix (Applied Biosystems, CA, USA), and 1 µL of 10 µM forward and reverse primers. qPCR assays were conducted under the following conditions: the temperature was held at 50 °C for 2 min and 95 °C for 10 min, followed by 40 cycles of 95 °C for 15 s, annealing at different temperatures (Table S1) for 15 s, and 72 °C for 30 s. Melt curve analysis was conducted for all SYBR® Green real-time PCR assays to verify the specificity of the primer.

PCR assays and agarose gel electrophoresis

PCR was conducted on a DNA thermocycler (Applied Biosystems, CA, USA) to amplify the *invA* and *purE* genes from the cDNA samples. Each 25-µL PCR reaction contained 2 µL of cDNA template, 1 µL of each primer from 10 µM stock, 12.5 µL of 2 × GoTaq®G2 Green Master Mix, and 8.5 µL PCR-grade sterile water. The PCR reaction was programmed for 5 min at 95 °C, followed by 30 cycles of 15 s at 95 °C, 15 s at annealing temperature (Table S1), and 30 s at 72 °C, with a final extension for 5 min at 72 °C. The PCR products were confirmed by agarose gel electrophoresis.

Standard curves of qPCR assays

The standard curves in the qPCR assays were achieved by serially diluting the plasmids containing each target gene (10^1 to 10^6 copies per reaction). The purified PCR products were ligated into the pGEM-T Easy Vector (Promega, USA), which was then cloned into JM109 competent cells. Plasmids containing the PCR amplicons were extracted using a QIAprep Spin Miniprep Kit (Qiagen, Valencia, CA, USA). The plasmid DNA concentration was quantified using the NanoDrop 2000 spectrophotometer. Standard curves were prepared using serial tenfold dilutions of the plasmid DNA containing each target gene.

Detection of *S.* Typhimurium on eggshell surface

Eggs with an average weight of approximately 50 g were purchased from a Singapore local market. Before the artificial contamination process, the eggshell was sterilized using 70% ethanol. Each egg was placed in 200 mL tryptic soy broth, inoculated with a single colony of *S.* Typhimurium from the overnight tryptic soy (Difco™, USA) agar plate and shaken at 60 rpm at 37 °C for 48 h in a laboratory shaking incubator.

After incubation, the eggs (replicate $n = 3$) used for UV treatment were placed in Petri dishes (one egg per Petri dish). Then, 1-h UV disinfection was conducted in a Type A2 Biological Safety Cabinet (BSC) equipped with a timed UV system (Thermo Scientific), and the eggs were turned every 15 min to other sides with fulfilled UV exposure. Meanwhile, another batch of three contaminated eggs was placed in sealed plastic bags (one egg in each bag) and subjected to pasteurization disinfection in a water bath at 60 ℃ for 15 min. The pasteurization condition was selected to avoid the denaturation of egg protein, since we incubate *S.* Typhimurium cells together with the whole egg. After the pasteurization disinfection, the plastic bags with eggs were immediately placed on ice to cool down before the following procedure. For control group, three contaminated eggs without any disinfection treatment were placed in parallel. Subsequently, *S.* Typhimurium was transferred from the surface of the eggs into 20 mL 1 × PBS buffer using three sterilized swabs sequentially to maximize the availability of *S.* Typhimurium cells. Next, DNA-intercalating dye treatments, DNA extraction, and qPCR assay were performed following the same procedures described above. For all experimental conditions, the loss of cell culturability was determined in triplicate by plate counting on TSA.

Data analysis

To evaluate the effects of PMA, DyeTox13, and DyeTox13 + EMA on the treated and untreated samples, we calculated ΔC_t values by subtracting the C_t value of the untreated samples from the C_t value of the dye-treated samples. The error bars in the figures of this study indicate the standard deviations from three independent biological replicates. Analysis of variance (ANOVA) and Tukey's test were applied to evaluate the significance of differences in $\Delta\Delta C_t$ using OriginPro 8.5. Also, the limit of detection (LOD) was determined via a serial dilution method to consider the C_t values for the disinfected samples (Ripp 1996; Desimoni and Brunetti 2015). To further understand the changes in the gene expression of *S.* Typhimurium after pasteurization and UV treatment, the gene expression levels of *invA* and *purE* genes were normalized using the cDNA concentrations from untreated samples with either pasteurization or UV disinfection.

Results

Optimization of the DyeTox13-qPCR assay for *S.* Typhimurium

To optimize the concentrations of the DyeTox13 and DyeTox13 with EMA addition (DyeTox13 + EMA) treatments, viable and heat-killed *S.* Typhimurium were treated with different EMA concentrations (10, 25, and 50 µM) while the DyeTox13 concentration remained at 50 µM. Figure 1 illustrates the effect of the different EMA concentrations on the DyeTox13-qPCR assay results for *S.* Typhimurium. As the EMA concentration increased in the dye treatments, the ΔC_t values of the viable (untreated) samples changed only slightly with no significant difference (p-value > 0.05). However, the heat-killed *S.* Typhimurium exposed to increasing EMA concentrations exhibited noticeably higher ΔC_t values (p-value < 0.05) (Fig. 1A). For example, the ΔC_t value increased from 8.77 to 10.98, 13.85, and 13.21 after adding EMA concentrations of 10, 25, and 50 µM, respectively. Figure 1 B illustrates the $\Delta\Delta C_t$ values calculated by subtracting the ΔC_t values of untreated samples from the ΔC_t values of heat-killed samples. Tukey's test showed a significantly

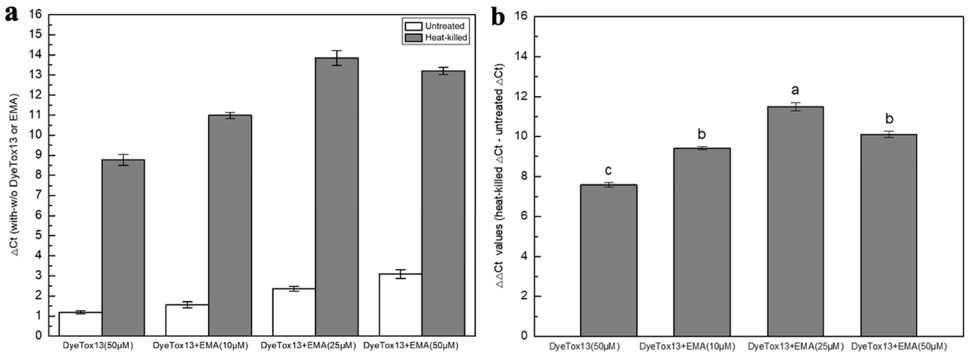

Fig. 1 Optimization of the DyeTox13-qPCR assay for *S.* Typhimurium. **A** results are shown as differences in ΔC_t values (with–w/o DyeTox13 Green C-2 Azide or/and EMA) by subtracting the C_t values of dye-untreated from the C_t values of dye-treated samples. (In the dye, DyeTox13 concentration remains 50 μM and the concentration of EMA increased gradually from 0 to 50 μM). **B** shows the differences in $\Delta\Delta C_t$ values (heat-killed ΔCt–untreated ΔC_t) by subtracting the ΔC_t values of untreated from the ΔC_t values of heat-killed samples. Alphabet placed on the top of columns presents the ANOVA distribution based on p-value < 0.005. The mean values and error bars were calculated from three independent replicates. Error bars indicate standard deviations of three independent biological repeats

higher $\Delta\Delta C_t$ value (p-value < 0.005) at the EMA concentration of 25 μM, indicating that the EMA treatment was complementary for reducing the PCR signals from dead cells, resulted in enhanced performance of the DyeTox13 treatment. Thus, we selected 25 μM EMA coupled with 50 μM DyeTox13 for further dye applications in the subsequent disinfection experiments.

The effects of pasteurization and UV disinfection on culturability, membrane integrity and metabolic activity of *S.* Typhimurium

The effects of pasteurization and UV treatment on *S.* Typhimurium were evaluated using a culture-dependent method (plate counting method) and viability PCR (PMA-qPCR, DyeTox13-qPCR, and DyeTox13 + EMA-qPCR). The pasteurization experiments were performed with different cell concentrations of *S.* Typhimurium. The ΔC_t values (with dyes minus without dyes) of untreated (non-pasteurized) samples under different cell concentrations were mostly in a range of 1 to 3 units with no significant difference (p-value > 0.05) according to the viability PCR assays (Fig. 2). The plate count results showed no culturable *S.* Typhimurium after the pasteurization treatment (Table S2), indicating that all *S.* Typhimurium lost their culturability. The results of DyeTox13-qPCR were comparable to those of PMA-qPCR under the pasteurization conditions at *S.* Typhimurium concentrations from 10^7 to 10^5 CFU/mL. Meanwhile, the addition of EMA to DyeTox13 significantly increased the ΔC_t values to 13.83 and 13.53 for the *S.* Typhimurium concentrations of 10^7 and 10^6 CFU/mL, respectively (p-value < 0.05), as shown in Fig. 2 A and B. However, when the *S. yphimurium* concentration was 10^5 CFU/mL, the ΔC_t values of the pasteurization treatment samples for the three different dye assays were 7.47, 7.91, and 6.17 for PMA, DyeTox13, and DyeTox13 + EMA, respectively (Fig. 2C). This can be attributed to the smaller amount of DNA extracted from the pasteurization samples and the C_t values being close to the limit of detection (LOD). Figure S2A shows the relative abundances of the different physiological statuses of *S.* Typhimurium measured by the three dye treatments (PMA, DyeTox13, and DyeTox13 + EMA), indicating that the condition of most of the cells was "membrane-compromised" after the pasteurization treatment.

Next, the effects of UV treatment on the viability of *S.* Typhimurium were examined. None of the culturable *S.* Typhimurium were detected via plate counting after UV treatment (Table S2), indicating that the UV exposure induced a non-culturable state of *S.* Typhimurium. The effects of UV disinfection at different doses caused the physiological states of *S.* Typhimurium shown in Fig. 2 D, E, and F. The ΔC_t values for all the non-UV-treated (untreated) samples were in the range of 1 to 2 units, and the PMA-qPCR results of *S. Typhimurium* for the samples exposed to UV treatment for the three exposure times were not significantly different (p-value > 0.05) from the ΔC_t values of the non-UV-treated results (Fig. 4). These PMA-qPCR results demonstrated that the membrane integrity of *S.* Typhimurium remained intact after UV treatment. However, considerably higher $\Delta C>_t$ values were observed with the DyeTox13 treatments (ΔC_t = 8.00, 8.90, and 9.45 for UV treatments of 10, 20, and 30 min, respectively). Furthermore, the addition of EMA to the DyeTox13 treatment led to even higher ΔC_t values (ΔC_t = 10.09, 12.16, and 12.65 for 10-, 20-, and 30-min exposures to UV, respectively). The addition of EMA improved DyeTox13's performance at determining the level of metabolic activity in the UV-treated cells by reducing the PCR signals from dead cells. Also, the pie chart indicated that high UV doses decreased the relative abundance of dormant cells and ABNC (active but not

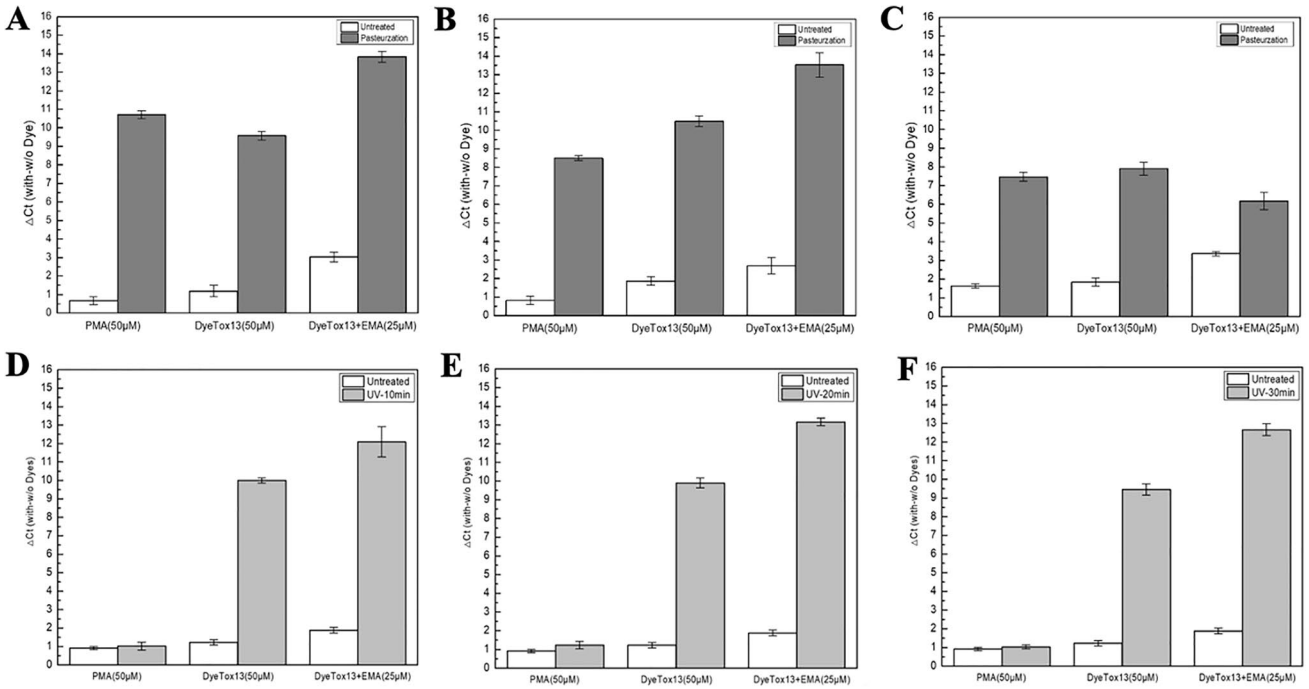

Fig. 2 Effect of pasteurization and UV exposure on bacteria viability measured by PMA, DyeTox13, and DyeTox13 + EMA-qPCR. **A**, **B** and **C** show the effect of pasteurization on different bacterial concentration: 10^7, 10^6, and 10^5 CFU/mL, respectively. **D**, **E** and **F** display the effect of different UV duration (10, 20 and 30 min) on *S.* Typhimurium, respectively. PMA, DyeTox13, and DyeTox13 + EMA treatment results are shown in ΔC_t (with-w/o dyes) based on PMA, DyeTox13, and DyeTox13 + EMA-qPCR analysis. The white and grey bars represent untreated and treated samples such as pasteurization and UV treatments, respectively. Error bars represent means and standard deviations, which were obtained in three independent biological replicates

culturable) in UV-treated samples (Figure S2B). Considering the CFU count and qPCR results for the DyeTox13 and DyeTox13 + EMA assays, most *S.* Typhimurium exposed to UV ceased their metabolic activities, and the relative abundance of membrane-compromised cells increased with the UV exposure time.

Evaluation of the disinfection treatment effect on gene expression levels in *S.* Typhimurium.

RT-qPCR measurements were used to analyze changes in gene expression levels caused by pasteurization and UV disinfection. The membrane-associated gene *invA* (invasion protein InvA) and the catalytic activity gene *purE* (phosphoribosylaminoimidazole carboxylase) of *S.* Typhimurium were selected in this study. RT-qPCR was used together with three DNA-intercalating dyes to understand the changes in the mRNA of *S.* Typhimurium as an indicator of physiological shifts during the disinfection treatments.

The effects of the two disinfectants on the transcripts coding invasion protein (*invA)* and biosynthesis (*purE*) were compared using the log2-fold changes. The log2-fold changes were calculated by normalizing the expressed transcripts for the samples with and without the pasteurization and UV irradiation treatments. The presence *invA* and *purE* was undetectable in pasteurization treatment sample via agarose gel electrophoresis (data not shown). The gene expression levels of cDNA (*invA and purE*) of the samples, which were exposed by PMA, DyeTox13, and DyeTox13 + EMA treatments, did not significantly differ because the concentrations of cDNA (*invA and purE*) were below the limit of detection or undetected (Fig. 3 A and B). Significant reductions of the gene expression level were observed based on differences in the log2 fold changes, ranging from − 6.5 to − 10.07. The gene expression levels corresponded with the results that pasteurization led to a membrane-compromised state and low proportion (less than 0.1%) of dormant and ABNC cells, as shown in Figure S2A. The cDNA of the *invA* genes without any dye treatment indicated relatively low fold changes at 10^7 CFU/mL of *S.* Typhimurium after pasteurization, while no gene expression of *purE* was detected in the samples treated with the DNA-intercalating dyes (Fig. 3B). Thus, the log2-fold changes of *invA* and *purE* indicated that pasteurization triggered disruption of both the cell membrane and the metabolic activity of *S.* Typhimurium.

UV irradiation significantly inhibited the gene expression of the *purE* gene, while *invA* transcripts persisted after the UV exposure except with the DyeTox13 (30 min only)

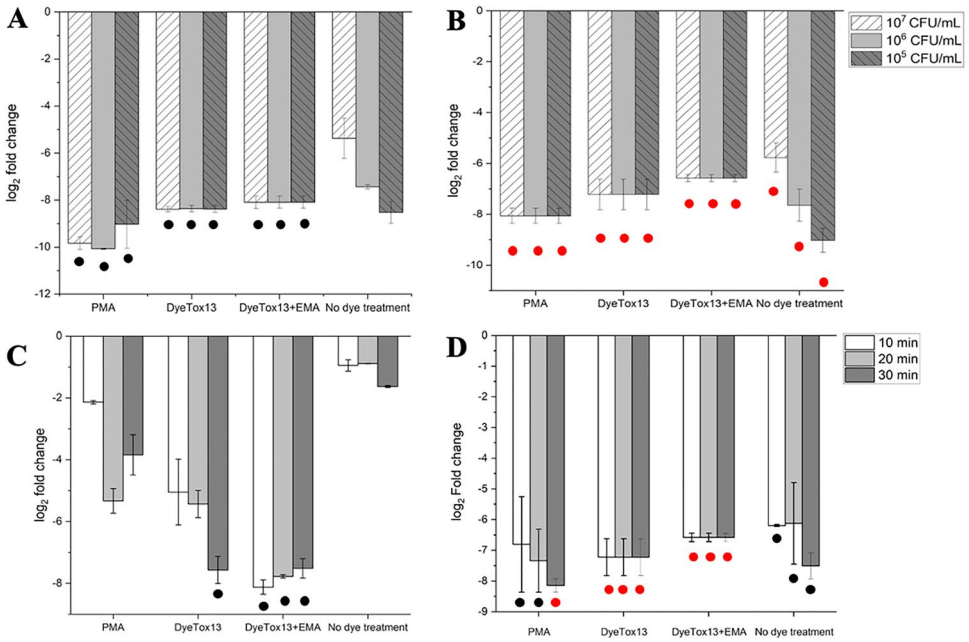

Fig. 3 The effect of pasteurization and UV treatment on the gene expression of *invA* and *purE* gene in *S.* Typhimurium measured by PMA, DyeTox13, DyeTox13+EMA assay, and no dye treatment. **A** and **B** show the log2-fold changes of *invA* (**A**) and *purE* (**B**) after of pasteurization. **C** and **D** present the log2-fold change of *invA* (**C**) and *purE* (**D**) after 10-min, 20-min, 30-min UV treatment, respectively. The fold changes were normalized by the expressed transcripts without any pasteurization and UV treatments. Error bars represent means and standard deviations, which were obtained in three independent biological replicates. Black and red dot indicate the gene expression below the limit of detection and non-detection after pasteurization and UV treatment, respectively

and DyeTox13 + EMA (all durations) treatments (Fig. 3 C and D). Yet, increasing intensity of the UV dose caused greater log2-fold changes of *invA* in the PMA, DyeTox13, and DyeTox13 + EMA treatments, whereas the changes in the *invA* gene were relatively insignificant under no dye treatment. As shown in Fig. 3C, the RT-qPCR revealed the presence of target cDNA in the UV-treated samples, even though the log2-fold change ranged from − 2.13 to − 5.53 for the PMA treatment. Also, the fold change values of the DyeTox13 and DyeTox13 + EMA assays were significantly higher than those of the PMA assay (p-value < 0.05), indicating that UV disinfection caused inhibition of metabolic activity and slight damage to the membrane. Significant differences in the gene expression of *purE* were observed, and most expression levels were under the limit of detection or were not detected (Fig. 3D). The disparity in the gene expression level between *invA* and *purE* demonstrated that while UV irradiation hindered catalytic activity, the membrane-associated protein gene *invA* was still expressed in UV-treated cells. Thus, the fold changes showed that cells maintained their membrane integrity but were metabolically inactive following the UV treatment. Also, continued gene expression of the *invA* gene could occur in UV-treated cells, indicating that the *invA* gene might not be a suitable target gene for the detection of metabolically active *Salmonella*.

vPCR assay of *S.* Typhimurium on the eggshell

No *S.* Typhimurium was detected on the control eggshell using the plate counting method, while the amount of *S.* Typhimurium ranged from 10^5 to 10^6 CFU on the non-disinfected eggshell after 48 h of incubation in a laboratory shaking incubator (Table S2). However, after pasteurization or UV disinfection, no *S.* Typhimurium was detected via the culture-based method. The ΔC_t values of heat-treated (pasteurized) *S.* Typhimurium that were artificially contaminated on eggshells showed significant differences among the PMA, DyeTox13, and DyeTox13 + EMA assays, with values of 2.98, 5.77, and 7.18, respectively (p-value < 0.05) (Fig. 4A). Figure 4 B shows that PMA could not effectively differentiate bacterial viability on eggshells after UV disinfection, as the ΔC_t value was 0.81 and was not significantly different from that of the non-UV-exposed samples. However, the ΔC_t values for the DyeTox13 and DyeTox13 + EMA assays were 4.96 and 5.83, respectively. Thus, the DyeTox13 treatment can identify the physiological states of bacteria after disinfection, particularly for UV exposure, which can interfere with metabolic activity without compromising the intact cell

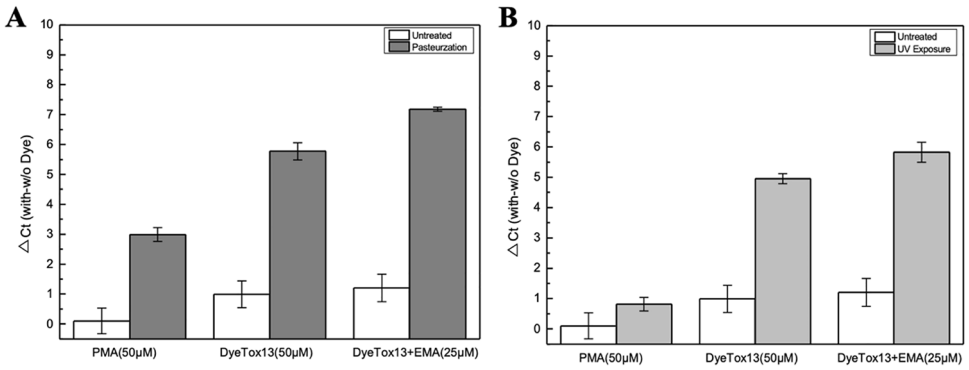

Fig. 4 Effect of pasteurization and 1 h-UV exposure on *S.* Typhimurium viability on eggshell surface measured by PMA, DyeTox13, and DyeTox13 + EMA-qPCR (*invA* gene). A and B show the results of pasteurization and UV treatment in viability qPCR assay, respectively. PMA, DyeTox13, and DyeTox13 + EMA assays results are shown in ΔC_t (with-w/o dyes) based on qPCR analysis. Error bars represent means and standard deviations, which were obtained in three independent biological replicates

membrane. Based on these findings, the DyeTox13 treatment could provide rapid detection of viable *S.* Typhimurium after pasteurization and UV disinfection. Furthermore, Fig. 4B also implies that the addition of EMA to DyeTox13 could improve the performance of DyeTox13 in the detection of *S.* Typhimurium on different environment matrices.

Discussion

In this study, viability measurements were performed using different viability methods: the plate counting method for cell culturability, DyeTox13-PCR for enzymatic activity as a proxy for metabolic activity in viable cells, and PMA-qPCR for membrane integrity. Specifically, we investigated changes in the physiological status of bacterial cells induced by pasteurization and UV disinfection because microbial populations might exhibit heterogeneous responses to these stressors.

To determine metabolic activity, we employed the DyeTox13 assay, a membrane-permeable DNA-intercalating dye, to identify cells with enzymatic activity (Lee and Bae 2018a, b). When DyTeox13 penetrates the cytoplasm, the intracellular esterase activity in a metabolically active cell ("ABNC" and "culturable alive" cells) hydrolyzes the dye's ester bonds. The DyeTox13 dye is thereby disabled from binding to nucleic acids. In contrast, in metabolically inactive cells, the dye retains its azide group and preferentially binds to intracellular nucleic acids during photoactivation, altering the structure of the nucleic acids to block its amplification during PCR. In this study, the addition of EMA to the DyeTox13-qPCR improved the dye's performance in differentiating viable from heat-killed cells. Since EMA is relatively permeant, EMA could penetrate viable cells to some extent (Seinige et al. 2014; Lee and Bae 2018a, b). However, we observed that the low-dose EMA treatment did not affect PCR amplification from live *S.* Typhimurium. In previous work, when treatment with PMA alone was insufficient to suppress the amplification from residual dead bacteria, the combination of PMA with EMA improved discrimination of live cells from dead cells (Minami et al. 2010). In our study, this was verified by significantly higher ΔC_t values (with–w/o dye) when the EMA concentration was at least 25 μM under the heat lysis condition (Fig. 1). The combination of DyeTox13 and low-dose EMA could enhance discrimination of enzymatically active cells from dead cell because PCR signals of extracellular enzyme activity from dead or membrane-compromised cell could be reduced by EMA treatment (Codony et al. 2015; Kiefer et al. 2020). In detail, DyeTox13 is based on intracellular esterase activity in cells. However, extracellular esterase could be present from membrane-compromised cells or dead cells. Thus, the membrane-impermeable EMA dye can improve DyeTox13 performance by reducing PCR signal from those cells that could retain esterase enzyme or extracellular esterase enzyme.

When applied to differentiate the physiological states of bacteria after disinfection treatments such as pasteurization and UV irradiation, this DyeTox13 assay could estimate subpopulation shifts in *S.* Typhimurium from alive to dead state, a process which contains many steps, as shown in Fig. 5. The microbial population can be classified into more diverse physiological statuses than "live" and "dead" (Davey 2011). Subpopulations of cells could be characterized on a spectrum from "live, actively metabolizing cell" to "dead" and, potentially, degraded (Fig. 5). Over the disinfection process, viability measurements based on culturability, metabolic activity, RNA and/or DNA content, and membrane permeability implied different physiological statuses in different individual cells. While the extreme cases (e.g., alive and dead) are relatively straightforward, the reversibility of these steps and the moment of death

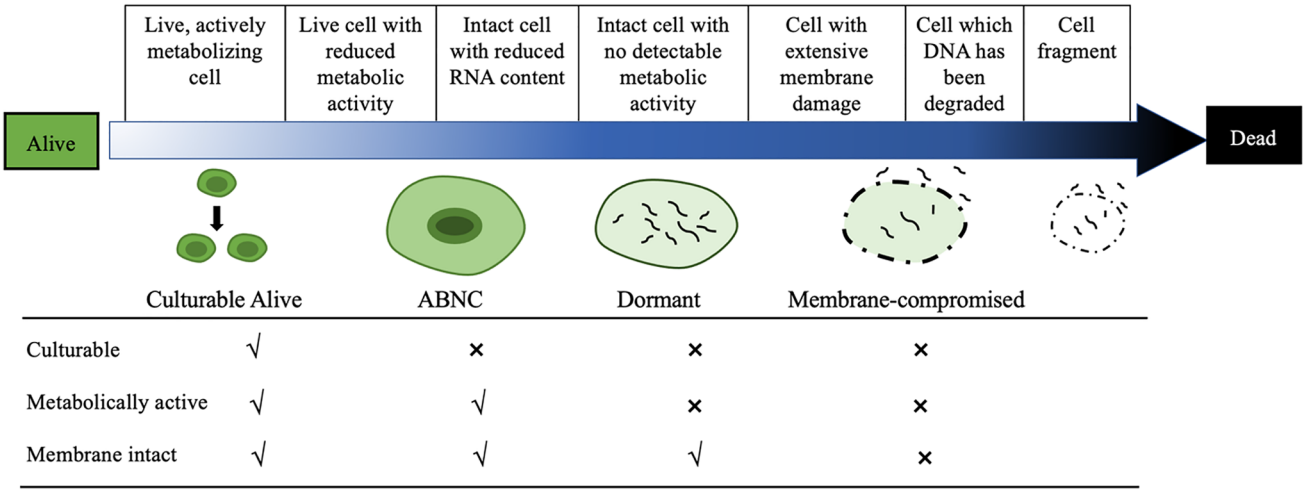

Fig. 5 The route from "live" to "dead" contains many steps containing different physiological states and the schematic representation of selected viability states and characteristics associated with three viability criteria. ABNV refers to "active but nonculturable"

are often difficult to define. For example, the mechanism of inactivation of bacteria during pasteurization is to disrupt the cell membrane and proteins through heat transfer for a specified duration (Wang et al. 2020). Thus, most of the *S.* Typhimurium after pasteurization moved toward a membrane-compromised state, while "ABNC" and "dormant" cells made up less than 1% of the total number of cells (Figure S2). Because the dominant cell status after pasteurization was extensive membrane damage, both the DyeTox13 and PMA treatments were capable of distinguishing alive and dead cells (Bae and Wuertz 2009; Liang et al. 2011).

Low UV doses have been reported to lead to negligible damage to the cell membrane, retaining the unimpaired integrity of the cell membranes but disrupting the cell's metabolic activities (Xu et al. 2018). Thus, aside from membrane integrity and culturability, metabolic activity might be considered as a meaningful viability criterion when determining the physiological state of the bacterium to differentiate the "ABNC" state and the "dormant" state in VBNC cells (Trevors 2012). While PMA can only bind to DNA in membrane-compromised cells, DyeTox13 penetrates the intact membrane of bacteria to bind to the DNA in enzymatically inactive cells and prevent DNA amplification (Nocker et al. 2006, Lee and Bae 2018a, b). Moreover, as the enzymatically active cells can hydrolyze to cleave the azide groups in DyeTox13, the cleaved azide group can be excluded via efflux pump, preventing the binding of DyeTox13 to the DNA (Lee and Bae 2018a, b). The high ΔC_t value in the DyeTox13 assay (Fig. 3) indicated that DyeTox13 was more capable of distinguishing UV-treated bacterial cells from non-UV (untreated)-treated cells. Furthermore, the DyeTox13-vPCR could provide insight into the changes in physiological states during the UV disinfection, implying that an increasing dose of UV irradiation gradually shifted the bacterial population from a "dormant" state to the "membrane-compromised" state (Fig. 5). Our study indicated that "ABNC" bacteria accounted for less than 0.1% of the total number of bacteria (Figure S2B).

Because of the shorter half-life of RNA relative to DNA, RNA-based assays have been used to detect living cells or recent pathogenic contaminations of foods (Techathuvanan and D'Souza 2020). Thus, RNA-based gene expression for two transcripts (*invA* and *pureE*) was also measured to determine different physiological states of cells under pasteurization and UV disinfection in this study. The main function of the *purE* gene is the translation of the enzyme involved in nucleotide biosynthesis, particularly for purine biosynthesis in metabolism (Meyer et al. 1992; Petersen et al. 1996). Meanwhile, the *invA* gene usually codes for a protein in the inner bacterial membrane that is responsible for the invasion of intestinal cells of the host. Also, the expression of the *invA* gene is more dependent on the cell's internal environment than on individual metabolic activities (Wang et al. 2009). The pasteurization treatments caused most of the cells to become membrane-compromised, as shown by the ΔC_t values from the PMA and DyeTox13 assays (Fig. 2). The overall tendency of the gene expressions of *invA* and *purE* also indicated that heat-treated cells entered a membrane-compromised state (Fig. 3 A and B).

mRNA has been a promising candidate as an indicator of viability in bacteria, but its persistence in dead cells depends on the inactivating treatment and subsequent holding conditions (Sheridan et al. 1998). The normalized gene expression levels of *purE* were significantly lower in UV-treated cells because the pyrimidines and purines can

absorb UV light, resulting in inhibition of purine biosynthesis (Sinha and Hader 2002). Interestingly, *invA* mRNA remained detectable under the low intensity of UV treatment with the PMA treatment and the no dye treatment. This could be explained by the mRNA transcripts that were being transcribed during the time of UV exposure not being destroyed or completely leaked from the cells. Also, continued gene expression after cell death might occur for limited periods of time in bacteria (Trevors 2012). The log2-fold changes of the DyeTox13 and DyeTox13 + EMA assays were significantly greater than that of PMA, indicating that permeable DyeTox13 can bind to the mRNA of metabolically inactive cells and subsequently inhibit cDNA synthesis. When a population of cells is exposed to stress, depending on the magnitude of the stress, there might be heterogeneous responses where some cells are killed, others are injured, and yet others may exhibit viability features such as reduced metabolic activity, reduced RNA content or intact cells with no detectable metabolic activity. In a mixed population composed of cells in different physiological states, as mentioned above, resuscitation stimulus could transition dormant to ABNC cells or allow injured cells to recover to an active state.

In our study, the PMA and DyeTox13 assays were applied to eggs artificially contaminated with pure-cultured *S.* Typhimurium, which were then treated by pasteurization and UV disinfection. The significant difference in ΔC_t values between DyeTox13 assay and PMA indicated that the *S. Typhimurium* on the eggshell entered the dormant state after pasteurization. Also, the ΔC_t values of the egg samples were observed to be significantly lower than those of suspended cultures. One reason for this could be the formation of a biofilm on the eggshell after a long incubation of the eggs with *S.* Typhimurium, where the biofilm itself could reduce the efficiency of heat transfer during pasteurization (Characklis, Nevimons et al. 1981). Also, the performance of the DNA-intercalating dyes could be hindered by the complex components swabbed from the eggshell because of potential interferences, such as ion concentrations, pH value, organic and inorganic ingredients, and chemical adsorption (Fittipaldi et al. 2012; Fang et al. 2018). Additionally, the DyeTox13 assay proved that "dormant" *S.* Typhimurium cells with no metabolic activity were prevalent in the eggshell samples after UV irradiation, whereas the PMA assay could only distinguish "membrane-compromised" cells. Thus, DyeTox13 can be applied to various disinfection methods, as disinfection achieved by different treatments can lead to distinct differences in the enzymatic activity as a proxy for metabolic activity and membrane permeability of the disinfected microbes (Blatchley et al. 2007). Therefore, the detection of metabolically inactive *S.* Typhimurium using the DyeTox13-qPCR assay could provide rapid identification of metabolically active cells and determine disinfection efficiency for food safety.

Supplementary Information The online version contains supplementary material available at https://doi.org/10.1007/s00253-022-11850-0.

Author contribution LL, FJ, and SB conceived and designed the research. LL conducted the experiment. LL, FJ, and SB wrote the manuscript. All the authors read and approved the manuscript.

Funding This work was supported by Technology Acceleration Programme (R-302–000-261–118) and a research grant from the Ministry of Education, Singapore, under AcRF Tier 1 (R-302–000-216–114).

Data availability All data generated or analyzed during this study are included in this published article and its supplementary information files.

Declarations

Ethics approval This article does not contain any studies with human participants or animals performed by any of the authors.

Conflict of interest The authors declare no conflict of interest for this work.

References

Aung KT, WC, Khor S, Octavia A, Ye J, Leo PP, Chan G, Lim WK, Wong BZ, Tan , Schlundt J, Dalsgaard A, Ng LC, Lin YN (2020). Distribution of *Salmonella* serovars in humans, foods, farm animals and environment, companion and wildlife animals in Singapore. Int J Environ Res Public Health. 17(16) https://doi.org/10.3390/ijerph17165774

Bae S, Wuertz S (2009) Rapid decay of host-specific fecal *Bacteroidales* cells in seawater as measured by quantitative PCR with propidium monoazide. Water Res 43(19):4850–4859. https://doi.org/10.1016/j.watres.2009.06.053

Bae, S., S. J. A. Wuertz and e. microbiology (2009). Discrimination of viable and dead fecal *Bacteroidales* bacteria by quantitative PCR with propidium monoazide. Appl Environ Microbiol. 75(9):2940-2944https://doi.org/10.1128/aem.01333-08

Blatchley ER, Gong WL, Alleman JE, Rose JB, Huffman DE, Otaki M, Lisle JT (2007) Effects of wastewater disinfection on waterborne bacteria and viruses. Water Environ Res 79(1):81–92. https://doi.org/10.2175/106143006x102024

Characklis WG, Nevimons M, Picologlou BJHEE (1981) Influence of fouling biofilms on heat transfer. Heat Transfer Eng. 3(1):23–37. https://doi.org/10.1080/01457638108939572

Chen SY, Wang F, Beaulieu JC, Stein RE, Ge BL (2011) Rapid detection of viable *Salmonellae* in produce by coupling propidium monoazide with loop-mediated isothermal amplification. Appl Environ Microbiol 77(12):4008–4016. https://doi.org/10.1128/aem.00354-11

Chiang E, Lee S, Medriano CA,Li L, Bae S (2021). Assessment of physiological responses of bacteria to chlorine and UV disinfection using a plate count method, flow cytometry and viability PCR. J Appl Microbiol. 2021 Oct 12 https://doi.org/10.1111/jam.15325

Codony F, Agustí G, Allué-Guardia AJM, c. probes, (2015) Cell membrane integrity and distinguishing between metabolically active

and inactive cells as a means of improving viability PCR. Mol Cell Probes 29(3):190–192. https://doi.org/10.1016/j.mcp.2015.03.003

Davey HM (2011) Life, death, and in-between: meanings and methods in microbiology. Appl Environ Microbiol 77(16):5571–5576. https://doi.org/10.1128/aem.00744-11

Desimoni E, Brunetti B (2015) About estimating the limit of detection by the signal to noise approach. Pharm Anal Acta 6:355. https://doi.org/10.4172/2153-2435.1000355

Fang J, Wu Y, Qu D, Ma B, Yu X, Zhang M, Han JJLIAM (2018) Propidium monoazide real-time loop-mediated isothermal amplification for specific visualization of viable Salmonella in food. Lett Appl Microbiol. 67(1):79–88. https://doi.org/10.1111/lam.12992

Fittipaldi M, Nocker A, Codony F (2012) Progress in understanding preferential detection of live cells using viability dyes in combination with DNA amplification. J Microbiol Methods 91(2):276–289. https://doi.org/10.1016/j.mimet.2012.08.007

Gunasekera TS, Sorensen A, Attfield PV, Sorensen SJ, Veal DA (2002) Inducible gene expression by nonculturable bacteria in milk after pasteurization. Appl Environ Microbiol 68(4):1988–1993. https://doi.org/10.1128/aem.68.4.1988-1993.2002

Ju WT, Moyne AL, Marco ML (2016) RNA-based detection does not accurately enumerate Living *Escherichia coli* O157:H7 cells on plants. Front Microbiol 7:223. https://doi.org/10.3389/fmicb.2016.00223

Karlinsey JE, Stepien TA, Mayho M, Singletary LA, Bingham-Ramos LK, Brehm MA, Greiner DL, Shultz LD, Gallagher LA, Bawn M, Kingsley RA, Libby SJ, Fang FC (2019). Genome-wide analysis of *Salmonella enterica* serovar typhi in humanized mice reveals key virulence featureS. Cell Host Microbe. 26(3):426-+ https://doi.org/10.1016/j.chom.2019.08.001

Kidgell C, Reichard U, Wain J, Linz B, Torpdahl M, Dougan G, Achtman M (2002) *Salmonella* typhi, the causative agent of typhoid fever, is approximately 50,000 years old. Infect Genet Evol 2(1):39–45. https://doi.org/10.1016/s1567-1348(02)00089-8

Kiefer A, Tang P, Arndt S, Fallico V, Wong C (2020) Optimization of viability treatment essential for accurate droplet digital PCR enumeration of probiotics. Front Microbiol 11:1811. https://doi.org/10.3389/fmicb.2020.01811

Kort, R., B. J. Keijser, M. P. M. Caspers, F. H. Schuren and R. Montijn (2008). Transcriptional activity around bacterial cell death reveals molecular biomarkers for cell viability. BMC Genomics. 9https://doi.org/10.1186/1471-2164-9-590

Lee S, Bae S (2018a) Evaluating the newly developed dye, DyeTox13 Green C-2 Azide, and comparing it with existing EMA and PMA for the differentiation of viable and nonviable bacteria. J Microbiol Methods 148:33–39. https://doi.org/10.1016/j.mimet.2018.03.018

Lee S, Bae S (2018b) Molecular viability testing of viable but non-culturable bacteria induced by antibiotic exposure. Microb Biotechnol 11(6):1008–1016. https://doi.org/10.1111/1751-7915.13039

Liang NJ, Dong J, Luo LX, Li Y (2011) Detection of viable *Salmonella* in lettuce by propidium monoazide real-time PCR. J Food Sci 76(4):M234–M237. https://doi.org/10.1111/j.1750-3841.2011.02123.x

Majowicz SE, Musto J, Scallan E, Angulo FJ, Kirk M, O'Brien SJ, Jones TF, Fazil A, Hoekstra RM, B Int Collaboration Enteric Dis (2010). The global burden of nontyphoidal *Salmonella* gastroenteritis. Clin Infect Dis. 50(6):882-889https://doi.org/10.1086/650733

Meyer E, Leonard NJ, Bhat B, Stubbe J, Smith JM (1992) Purification and characterization of the pure, PURK, and PURC gene-products - identification of a previously unrecognized energy requirement in the purine biosynthetic-pathway. Biochemistry 31(21):5022–5032. https://doi.org/10.1021/bi00136a016

Minami J, Yoshida K, Soejima T, Yaeshima T, Iwatsuki K (2010) New approach to use ethidium bromide monoazide as an analytical tool. J Appl Microbiol 109(3):900–909. https://doi.org/10.1111/j.1365-2672.2010.04716.x

Nocker A, Cheung CY, Camper AK (2006). Comparison of propidium monoazide with ethidium monoazide for differentiation of live vs. dead bacteria by selective removal of DNA from dead cells. J Microbiol Methods. 67(2):310–320 https://doi.org/10.1016/j.mimet.2006.04.015

Petersen L, EnosBerlage J, Downs DM (1996) Genetic analysis of metabolic crosstalk and its impact on thiamine synthesis in *Salmonella typhimurium*. Genetics 143(1):37–44

Ripp J (1996) Analytical detection limit guidance and laboratory guide for determining method detection limits. Wisconsin Department of Natural Resources Laboratory Certification Program Report No. PUBL-TS-056-96. Madison, WI, USA, p 30

Rodriguez-Lazaro D, Hernandez M, D'Agostino M, Cook N (2006) Application of nucleic acid sequence-based amplification for the detection of viable foodborne pathogens: progress and challenges. J Rapid Methods Autom Microbiol 14(3):218–236. https://doi.org/10.1111/j.1745-4581.2006.00048.x

Sánchez-Vargas FM, Abu-El-Haija MA, Gómez-Duarte OGJTm and I disease (2011). *Salmonella* infections: an update on epidemiology, management, and prevention. Travel Med Infect Dis. 9(6):263-277https://doi.org/10.1016/j.tmaid.2011.11.001

Seinige D, Krischek C, Klein G, Kehrenberg C (2014) Comparative analysis and limitations of ethidium monoazide and propidium monoazide treatments for the differentiation of viable and nonviable *Campylobacter* cells. Appl Environ Microbiol 80(7):2186–2192. https://doi.org/10.1128/aem.03962-13

Sheridan GEC, Masters CI, Shallcross JA, Mackey BM (1998) Detection of mRNA by reverse transcription PCR as an indicator of viability in *Escherichia coli* cells. Appl Environ Microbiol 64(4):1313–1318. https://doi.org/10.1128/AEM.64.4.1313-1318.1998

Sinha RP, Hader DP (2002) UV-induced DNA damage and repair: a review. Photochem Photobiol Sci 1(4):225–236. https://doi.org/10.1039/b201230h

Techathuvanan C, D'Souza DH (2020) Propidium monoazide for viable *Salmonella enterica* detection by PCR and LAMP assays in comparison to RNA-based RT-PCR, RT-LAMP, and culture-based assays. J Food Sci 85(10):3509–3516. https://doi.org/10.1111/1750-3841.15459

Trevors JT (2011) Viable but non-culturable (VBNC) bacteria: Gene expression in planktonic and biofilm cells. J Microbiol Methods 86(2):266–273. https://doi.org/10.1016/j.mimet.2011.04.018

Trevors JT (2012) Can dead bacterial cells be defined and are genes expressed after cell death? J Microbiol Methods 90(1):25–28. https://doi.org/10.1016/j.mimet.2012.04.004

Wang X, X. Y. Zhai, H. R. Zhang, X. Y. Zhang, D. F. Ren and J. Lu (2020). Impact of ultra high pressure on microbial characteristics of rose pomace beverage: a comparative study against conventional heat pasteurization. LWT-Food Sci Technol 127https://doi.org/10.1016/j.lwt.2020.109395

Wang YP, Li L, Shen JZ, Yang FJ, Wu YN (2009) Quinolone-resistance in *Salmonella* is associated with decreased mRNA expression of virulence genes invA and avrA, growth and intracellular invasion and survival. Vet Microbiol 133(4):328–334. https://doi.org/10.1016/j.vetmic.2008.07.012

World Health, O. (2021). Food systems for health: information brief. Geneva, World Health Organization

Xu LM, Zhang CM, Xu PC, Wang XCC (2018) Mechanisms of ultraviolet disinfection and chlorination of *Escherichia coli*: culturability, membrane permeability, metabolism, and genetic

damage. J Environ Sci 65:356–366. https://doi.org/10.1016/j.jes.2017.07.006

Yang QR, Domesle KJ, Ge BL (2018) Loop-mediated isothermal amplification for *Salmonella* detection in food and feed: current applications and future directions. Foodborne Pathog Dis 15(6):309–331. https://doi.org/10.1089/fpd.2018.2445

Zhang SH, Ye CS, Lin HR, Lv L, Yu X (2015) UV disinfection induces a Vbnc state in *Escherichia coli* and *Pseudomonas aeruginosa*. Environ Sci Technol 49(3):1721–1728. https://doi.org/10.1021/es505211e

Zhao, X. H., J. L. Zhong, C. J. Wei, C. W. Lin and T. Ding (2017). Current perspectives on viable but non-culturable state in foodborne pathogens. Front Microbiol. 8https://doi.org/10.3389/fmicb.2017.00580